

TopoDiff: A Performance and Constraint-Guided Diffusion Model for Topology Optimization

François Mazé¹, Faez Ahmed¹

¹Massachusetts Institute of Technology
francois.maze@etu.minesparis.psl.eu, {fmaze,faez}@mit.edu

Abstract

Structural topology optimization, which aims to find the optimal physical structure that maximizes mechanical performance, is vital in engineering design applications in aerospace, mechanical, and civil engineering. Generative adversarial networks (GANs) have recently emerged as a popular alternative to traditional iterative topology optimization methods. However, these models are often difficult to train, have limited generalizability, and due to their goal of mimicking optimal topologies, neglect manufacturability and performance objectives like mechanical compliance. We propose TopoDiff, a conditional diffusion-model-based architecture to perform performance-aware and manufacturability-aware topology optimization that overcomes these issues. Our model introduces a surrogate model-based guidance strategy that actively favors structures with low compliance and good manufacturability. Our method significantly outperforms a state-of-art conditional GAN by reducing the average error on physical performance by a factor of eight and by producing 11 times fewer infeasible samples. By introducing diffusion models to topology optimization, we show that conditional diffusion models have the ability to outperform GANs in engineering design synthesis applications too. Our work also suggests a general framework for engineering optimization problems using diffusion models and external performance and constraint-aware guidance.

1 Introduction

Structural topology optimization (TO) of solid structures consists in generating the optimal shape of a material by minimizing an objective function, for instance, mechanical compliance, within a given domain and under a given set of constraints (volume fraction, boundary conditions, and loads). TO is therefore becoming an essential design tool and is now included in most professional design software (Autodesk, Solidworks). It is the driving force behind Autodesk’s generative design toolset, where designers input design goals into the software, along with parameters such as performance or spatial requirements, materials, manufacturing methods, and cost constraints. The software quickly generates design alternatives. Most methods to solve TO rely on gradient-based approaches, the most common method being the Solid Isotropic Material with Penalization method (Bendsøe and Kikuchi 1988; Rozvany, Zhou, and Birker 1992). Despite their wide adoption, these

traditional methods have two major pitfalls: they are computationally expensive, and they may generate non-optimal designs, mainly when some penalization and filtering augmentations are used to avoid grayscale pixels (Sigmund and Maute 2013).

Several deep learning methods have been developed in recent years to improve and speed up the TO process (Yu et al. 2018; Sharpe and Seepersad 2019; Nie et al. 2021; Behzadi and Ilieş 2021) by learning from large datasets of optimized topologies. The latest and most promising results were obtained with deep generative models (DGMs) and notably with conditional generative adversarial networks (cGANs) trained for image synthesis. Although very promising, most of these models train for visual similarity and do not model the physical performance of the generated structures. Most of them produce disconnected, floating material that seriously affects the manufacturability of the generated design. They also suffer from a low generalization ability, especially to out-of-distribution boundary conditions.

We hypothesize that these issues are caused by the absence of explicit guidance methods toward designs with low compliance and good manufacturability. We hypothesize that the reliance of the optimization objective on the sole cGAN prompts the model only to mimic pixel-wise the ground truth produced by traditional TO methods. Two images which differ little in pixel-wise similarity may still have extremely different performance values. The absence of explicit external guidance is even more problematic since the ground truth data is not guaranteed to be optimal, as explained above.

In this paper, we introduce TopoDiff, a conditional diffusion-model-based method for TO. Dhariwal and Nichol (2021) have shown that diffusion models can outperform GANs for image generation and diffusion models are easier to train - and therefore to adapt to other tasks - than GANs. In addition, the sequential nature of diffusion models makes them compatible with external guidance strategies that assist with performance and feasibility goals. By creating surrogate models to estimate performance, we thus introduce external guidance strategies to minimize mechanical compliance and improve manufacturability in diffusion models.

Our main contributions include: 1. A new diffusion model, TopoDiff, for Topology Optimization, that achieves an eight-times reduction in the average physical perfor-

mance error and an 11-times reduction in infeasibility; 2. A new guidance strategy for diffusion models to perform physical performance optimization; 3. A general framework to solve engineering problems using diffusion models, where sample feasibility and performance are important to model.

2 Background and Related Work

2.1 Topology Optimization

Topology Optimization (TO) finds an optimal subset of material Ω_{opt} included in the full design domain Ω under a set of displacement boundary conditions and loads applied on the nodes of the domain and a volume fraction condition. The solution is said to be optimal because it minimizes an objective function under these constraints. The most common objective function is mechanical compliance. Fig. 1 summarizes the principle of TO.

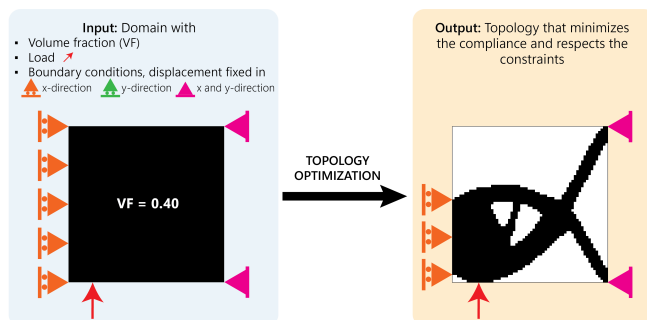


Figure 1: For a given set of load, boundary conditions and volume fraction, Topology Optimization (TO) aims to find the optimal structure that minimizes desired objectives such as compliance.

Traditional TO methods rely on Finite Elements Analysis (FEA). One popular method is the SIMP method, for Solid Isotropic Material with Penalization (Bendsøe and Kikuchi 1988; Rozvany, Zhou, and Birker 1992).

SIMP associates every element of the mesh with a *continuous* density to be able to perform gradient-based methods (Sigmund 2001). However, because intermediary densities make no physical sense, SIMP uses a penalization factor p to encourage binary densities in the Young modulus formula $E_i(y_i) = E_{min} + y_i^p (E_0 - E_{min})$ used in SIMP.

This penalization strategy (with $p > 1$) is efficient but introduces non-convexity in the objective function, as stated by Sigmund and Maute (2013). As a result, SIMP is likely to converge towards local optima. Other techniques used to encourage binary densities include filters, but they also introduce non-convexity (Sigmund and Maute 2013).

2.2 Deep Learning for Topology Optimization

Because of the FEA steps they include, traditional TO methods are computationally expensive and, therefore, time-consuming (Amir and Sigmund 2011). To improve speed and to address the non-convexity issue, some deep learning methods have recently been developed.

Some of these methods were designed to be used within a traditional gradient-based TO process. For instance, Guo

et al. (2018) use a variational auto-encoder (VAE) to represent topologies in a low-dimension latent space. They then run traditional TO in this latent space, which speeds up the optimization and improves the quality of the result. Lin et al. (2018) propose a convolutional neural network (CNN) that needs to be combined with traditional TO to speed up the optimization. Sosnovik and Oseledets (2019) state the TO problem as a classification problem by using a CNN to predict the final binary image from two halfway grayscale images generated by SIMP.

Another group of approaches to which our work belongs consists in proposing an end-to-end TO framework, from the constraints to the optimal topology. Thus, Yu et al. (2018) propose an iteration-free method, which predicts a low-resolution solution with a CNN encoder-decoder, which is then passed into a GAN to increase the resolution. In line with the work by Rawat and Shen (2019), Li et al. (2019) use two GANs to solve the TO problem and then predict the refined structure at high resolution. Sharpe and Seepersad (2019) introduce conditional GANs as a means of generating a compact latent representation of structures resulting from TO. Their work is improved by Nie et al. (2021) who greatly extend the generalizability in their model named Topology-GAN, which is trained on more diverse conditions and uses physical fields as input instead of raw matrices and vectors to represent loads and boundary conditions. In parallel, Wang et al. (2021) develop a U-Net to perform TO and show that it has some capacity of generalization. These two promising models nevertheless show a limited ability of generalization, notably regarding boundary conditions outside the training distribution. They are also both prone to the problem of disconnected material. In order to solve this issue, Behzadi and Ilieş (2021) propose another conditional GAN architecture that includes a topological measure of connectivity in its loss function. Their results are promising and seem to improve generalizability and connectivity, however, they set the volume fraction to a constant value, which limits the scope of the problem.

It is crucial to note that none of these methods explicitly include a process to minimize compliance, which is the goal of TO. The minimization of compliance is expected indirectly through the GAN training, which is by nature challenging to control and leads to limited generalization ability in practice. Incorporating some measure of predicted structural performance inside a conditional model seems necessary. To add explicit guidance towards low-compliance and good-feasibility structures, we use diffusion models.

2.3 Diffusion Models

Diffusion models are a new type of deep generative models (DGMs) introduced by Sohl-Dickstein et al. (2015). They have received much attention recently because Dhariwal and Nichol (2021) showed that diffusion models outperform GANs for image synthesis. Diffusion models are increasingly being applied to various fields: image generation (Nichol and Dhariwal 2021), segmentation (Amit et al. 2021), image editing (Meng et al. 2021), text-to-image (Nichol et al. 2021; Kim and Ye 2021), etc.

The idea behind diffusion models is to train a neural net-

work to reverse a noising process that maps the data distribution to a white noise distribution. The forward noising process, which is fixed, consists in progressively adding noise to the samples following the Markov chain:

$$q(x_t|x_{t-1}) = \mathcal{N}(x_t; \sqrt{\alpha_t}x_{t-1}, (1 - \alpha_t)I) \quad (1)$$

where $(\alpha_t)_{t=1}^T$ is a variance schedule.

To reverse this noising process, we approximate the true posterior with the parametric Gaussian process:

$$p_\theta(x_{t-1}|x_t) = \mathcal{N}(\mu_\theta(x_t), \Sigma_\theta(x_t)). \quad (2)$$

We then generate new data by sampling an image from $\mathcal{N}(0, I)$ and gradually denoising it using Eq. 2.

Training a diffusion model, therefore, consists in training two neural networks, $\mu_\theta(x_t)$ and $\Sigma_\theta(x_t)$, to predict the mean and the variance of the denoising process respectively. Let us note however that Ho, Jain, and Abbeel (2020) showed that $\Sigma_\theta(x_t)$ might be fixed to a constant instead of being learned.

2.4 Guidance Methods in Diffusion Models

A few guidance methods have been developed to perform conditional image generation, in particular, to include class labels when the model tries to generate an image corresponding to a given class.

Including conditioning information inside the denoising networks

A first method to condition a diffusion model consists in adding the conditioning information (for example, a class label) as an extra input to the denoising networks μ_θ and Σ_θ . In practice, the conditioning information can be added as an extra channel to the input image. Similarly, Dhariwal and Nichol (2021) suggest adding conditioning information into an adaptive group normalization layer in every residual block.

Classifier guidance Additional methods have been developed to guide the denoising process using classifier output. In line with Sohl-Dickstein et al. (2015) and Song et al. (2020) who have used external classifiers to guide the denoising process, Dhariwal and Nichol (2021) introduce *classifier guidance* to perform class-conditional image generation. In *classifier guidance*, a separate classifier is trained on noisy data (with different levels of noise) to predict the probability $p_\phi(y|x_t)$ that an image x_t at noise level t corresponds to the class y . Let $p_\theta(x_t|x_{t+1})$ be an unconditional reverse noising process. Classifier guidance consists in sampling from:

$$p_{\theta,\phi}(x_t|x_{t+1}, y) = Z p_\theta(x_t|x_{t+1}) p_\phi(y|x_t) \quad (3)$$

instead of $p_\theta(x_t|x_{t+1})$, where Z denotes a normalizing constant. Under reasonable assumptions, Dhariwal and Nichol (2021) show that sampling from $p_{\theta,\phi}(x_t|x_{t+1}, y)$ is equivalent to perturbing the mean with the gradient of the probability predicted by the classifier. Specifically, the perturbed mean is:

$$\hat{\mu}_\theta(x_t) = \mu_\theta(x_t) + s \Sigma_\theta(x_t) \nabla_{x_t} \log p_\phi(y|x_t) \quad (4)$$

where s is a scale hyperparameter that needs to be tuned.

A variant called classifier-free guidance was proposed by Ho and Salimans (2021). This technique is theoretically close to classifier guidance, but does not require training a separate classifier on noisy data.

However, none of these methods employ guidance for both continuous values (such as performance obtained from regression models) and discrete values (such, as class labels obtained from classification models), which is important for TO to achieve both high-performing and feasible samples.

3 Method

3.1 Architecture and General Pipeline

TopoDiff’s diffusion architecture consists of a UNet (Ronneberger, Fischer, and Brox 2015)-based denoiser at every step with attention layers, similar to Dhariwal and Nichol (2021). We add conditioning to this architecture by including information on constraints and boundary conditions as additional channels to the input image given to the denoiser, as shown in Figure 2. The UNet model uses these extra channels as additional information to denoise the first channel of the input in a way that respects the constraints and is optimal for the given boundary conditions. Similarly to TopologyGAN (Nie et al. 2021), we use physical fields, namely strain energy density and von Mises stress, to represent constraints and boundary conditions. The physical fields are computed using a finite element method (Guarín-Zapata and Gómez 2020). The final input to our conditional diffusion model has four channels representing the volume fraction, the strain energy density, the von Mises stress, and the loads applied to the boundary of the domain. We use physical fields because they add insightful information that can be used by the denoiser and additionally avoid the sparsity problem caused by raw constraints and boundary condition matrices.

3.2 Minimizing compliance

Most deep learning models used for TO rely on the objective to minimize the pixel-wise error between the output topology and the ground truth obtained with traditional methods. For instance, the reference model TopologyGAN (Nie et al. 2021) essentially tries to mimic the ground truth topology and is encouraged to do so by the L2 loss function of its generator. Most GANs for TO are evaluated using mean absolute error (MAE) between the ground truth topology and the topology predicted by their model. Yet, we hypothesize that setting the minimization of a pixel-wise error as an objective does not properly address the aim of TO: generate manufacturable structures that minimize mechanical compliance. We make this hypothesis for two main reasons:

1. The topology used as ground truth is generally not optimal because of penalization factor and filters (Sec. 2.1);
2. A small pixel-wise error is compatible with a large compliance error if the material is missing at critical places.

Without any additional guidance, our conditional diffusion model is prone to the same problem. To solve that issue, we introduce a new type of guidance called *regressor guidance*, inspired by the *classifier guidance* proposed by Sohl-Dickstein et al. (2015), Song et al. (2020) and Dhariwal and Nichol (2021).

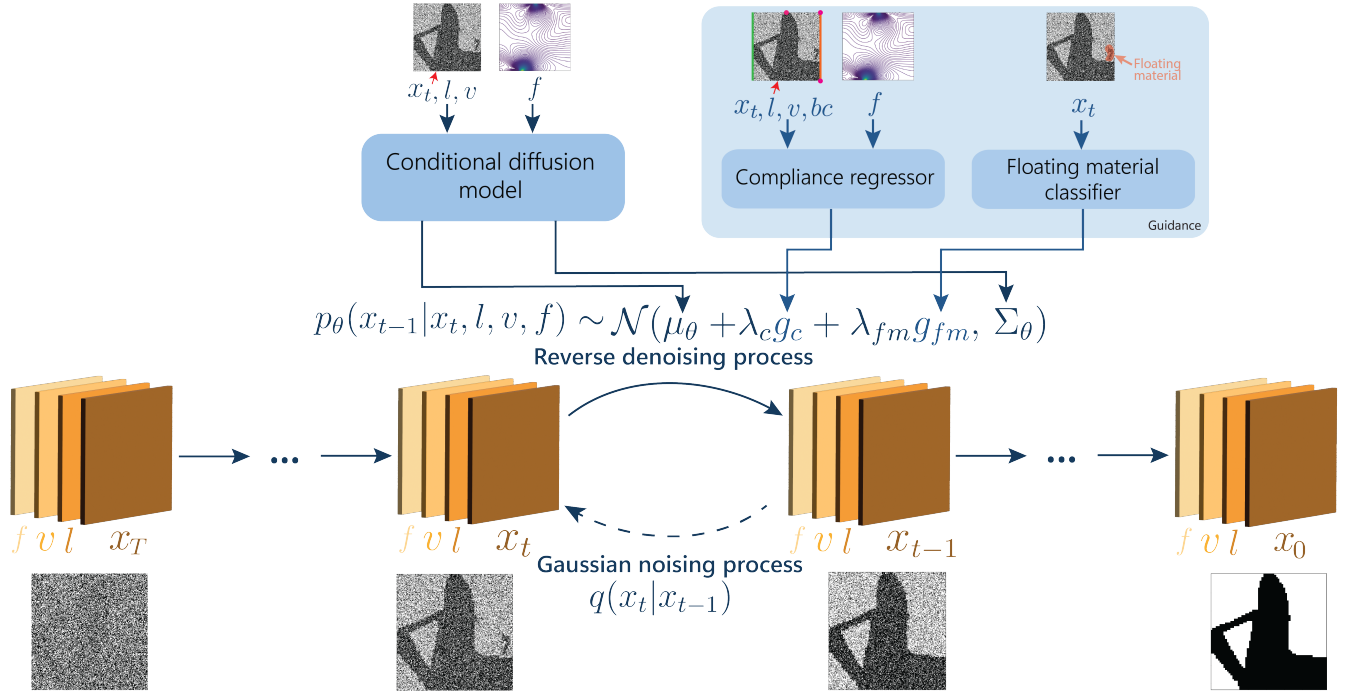


Figure 2: TopoDiff: Proposed constrained guided conditional diffusion model architecture for TO. $(x_t)_{t=0, \dots, T}$ is the gradually denoised topology; g_c and g_{fm} are the guidance gradients; l is the load applied, represented with a red arrow on the topology; v is the volume fraction; f are the physical fields and bc are the boundary conditions, represented with color lines and dots.

Consider a conditional diffusion model as presented in Sec. 3.1: $p_\theta(x_t|x_{t+1}, v, f, l)$, where v is the *volume fraction*, f are the physical fields (strain energy density and von Mises stress) and l are the loads applied. *Regressor guidance* consists in sampling each transition according to:

$$p_{\theta, \phi}(x_t|x_{t+1}, v, f, l, bc) = \frac{1}{Z} p_\theta(x_t|x_{t+1}, v, f, l) e^{-c_\phi(x_t, v, f, l, bc)} \quad (5)$$

where c_ϕ is a surrogate neural network predicting the compliance of the topology under given constraints, bc are the boundary conditions applied, and Z is a normalizing constant. It is worth noting that c_ϕ must be able to predict the compliance on noisy images of topologies. In order to perform this task, we use the encoder of a UNet architecture modified for regression values.

We show in Sec. 3.5 that under simple assumptions, adding *Regressor guidance* simply amounts to shifting the mean predicted by the diffusion model by $-\Sigma \nabla_{x_t} c_\phi(x_t, v, f, l, bc)$ where Σ is the variance of the Gaussian distribution representing $p_\theta(x_t|x_{t+1}, v, f, l)$.

This method thus modifies the distribution according to which we sample at every step by penalizing topologies with high compliance. The resulting algorithm is Alg. 1.

3.3 Avoiding Floating Material

Disconnected pixels in predicted topologies are a serious problem since this phenomenon leads to floating material and therefore affects the manufacturability of the predicted topology. This problem is generally ignored in deep learning

Algorithm 1 Regressor guidance for TO, given a conditional diffusion model $(\mu_\theta(x_t|x_{t+1}, v, f, l), \Sigma_\theta(x_t|x_{t+1}, v, f, l))$ and a regressor $c_\phi(x_t, v, f, l, bc)$.

Require: v, l, bc \triangleright Volume, loads and boundary conditions
Require: f \triangleright Physical fields
Require: λ_c \triangleright Regressor gradient scale

$x_T \leftarrow$ sample from $\mathcal{N}(0, I)$
for t from T to 1 **do**
 $\mu, \Sigma \leftarrow \mu_\theta(x_t|x_{t+1}, v, f, l), \Sigma_\theta(x_t|x_{t+1}, v, f, l)$
 $x_{t-1} \leftarrow$ sample from $\mathcal{N}(\mu - \lambda_c \Sigma \nabla_{x_t} c_\phi(x_t, v, f, l, bc)|_{x_t=\mu}, \Sigma)$
return x_0

models for TO, and is notably not taken into account by the pixel-wise error since a small pixel-wise error is compatible with the presence of floating material.

Similar to what has been exposed in Sec. 3.2, we further modify the sampling distribution at every step by penalizing topologies that contain floating material.

To do so, we train a classifier p_γ that returns the probability that the topology does *not* contain floating material. We then use this classifier to perform *classifier guidance*, as introduced in Sec. 2.4.

Eventually, this amounts to shifting the mean predicted by the diffusion model by $+\Sigma \nabla_{x_t} \log p_\gamma(x_t)$.

3.4 Combining Guidance Strategies

In the end, our model consists of one conditional diffusion model $p_\theta(x_t|x_{t+1}, v, f, l)$ and two surrogate models used

for guidance when sampling: $c_\phi(x_t, v, f, l, bc)$ for compliance and $p_\gamma(x_t)$ for floating material.

One challenge is to find a way to combine these two guidance strategies. To combine them, we sample at every step according to:

$$p_{\theta, \phi, \gamma}(x_t | x_{t+1}, v, f, l, bc) = Z p_\theta(x_t | x_{t+1}, v, f, l) e^{-c_\phi(x_t, v, f, l, bc)} p_\gamma(x_t). \quad (6)$$

This amounts to shifting the mean predicted by the diffusion model by:

$$-\lambda_c \Sigma \nabla_{x_t} c_\phi(x_t, v, f, l, bc) + \lambda_{fm} \Sigma \nabla_{x_t} \log p_\gamma(x_t) \quad (7)$$

where λ_c and λ_{fm} are gradient scale hyperparameters.

However, as is, this approach has two pitfalls: 1. The gradients are always computed at the same point μ (the mean predicted by the diffusion model), even though this mean is shifted by the previous guidance strategy; 2. The gradients are computed at every denoising step, even if we might want to favor one guidance over the other at a given denoising step. To address these issues, we modify the point at which the second gradient is computed by considering the shift induced by the previous gradient. In addition, we determine a maximum level of noise (MLN) beyond which the *classifier/regressor guidance* should not be included for every classifier and regressor. We then introduce *classifier/regressor guidance* only if the image is denoised enough to have a noise level below the MLN of the given classifier or regressor.

The final guidance algorithm resulting from the combination of these guidance strategies is Alg. 2. Fig. 2 also summarizes the overall architecture.

Algorithm 2 Guidance strategy for TO using Conditional Diffusion Model.

Require: $v, l, bc \triangleright$ Volume, loads and boundary conditions
Require: $f \triangleright$ Physical fields
Require: $\lambda_c, \lambda_{fm} \triangleright$ Regressor and classifier gradient scale
Require: $MLN_c, MLN_{fm} \triangleright$ Maximum levels of noise
 $x_T \leftarrow$ sample from $\mathcal{N}(0, I)$
for t from T to 1 **do**
 $\mu, \Sigma \leftarrow \mu_\theta(x_t | x_{t+1}, v, f, l), \Sigma_\theta(x_t | x_{t+1}, v, f, l)$
 if $t < MLN_{fm}$ **then**
 $\mu \leftarrow \mu + \lambda_{fm} \Sigma \nabla_{x_t} \log p_\gamma(x_t) |_{x_t=\mu}$
 if $t < MLN_c$ **then**
 $\mu \leftarrow \mu - \lambda_c \Sigma \nabla_{x_t} c_\phi(x_t, v, f, l, bc) |_{x_t=\mu}$
 $x_{t-1} \leftarrow$ sample from $\mathcal{N}(\mu, \Sigma)$
return x_0

It should be noted that we also considered applying *regressor* and *classifier guidance* for other constraints (volume, load position) but the conditional diffusion model already respects well these constraints and made guidance unnecessary.

3.5 Mathematical Motivations for Regressor Guidance

Similarly to Dhariwal and Nichol (2021) about *classifier guidance*, we show in this section the mathematical motiva-

tions behind *regressor guidance*, and in particular, we prove that adding *regressor guidance*, i.e., sampling each transition according to the modified distribution, amounts to a shift in the mean predicted by the diffusion model.

Let $p_\theta(x_t | x_{t+1}, v, f, l)$ be our conditional diffusion model. *Regressor guidance* consists in sampling according to:

$$p_{\theta, \phi}(x_t | x_{t+1}, v, f, l, bc) = Z p_\theta(x_t | x_{t+1}, v, f, l) e^{-c_\phi(x_t, v, f, l, bc)} \quad (8)$$

where Z is a normalizing constant and all variables are the ones defined in Sec. 3.2.

Let μ and Σ be the mean and variance of the Gaussian distribution representing $p_\theta(x_t | x_{t+1}, v, f, l)$.

$$\log p_\theta(x_t | x_{t+1}, v, f, l) = -\frac{1}{2}(x_t - \mu)^T \Sigma^{-1}(x_t - \mu) + C \quad (9)$$

where C is a constant.

By doing a Taylor expansion of the regressor predicting the compliance $c_\phi(x_t, v, f, l, bc)$, we obtain:

$$c_\phi(x_t, v, f, l, bc) \approx c_\phi(\mu, v, f, l, bc) + (x_t - \mu)^T \nabla_{x_t} c_\phi(x_t, v, f, l, bc) |_{x_t=\mu}. \quad (10)$$

In Eq. 10, we neglect the terms of second order and above because we make the assumption that the curvature of $c_\phi(x_t)$ is low compared to Σ^{-1} , to which it will be summed in Eq. 11. This assumption is reasonable in the limit of infinite diffusion steps, where $\|\Sigma\| \rightarrow 0$, as stated by Dhariwal and Nichol (2021).

Hence, Eq. 10 can be rewritten $c_\phi(x_t, v, f, l, bc) \approx (x_t - \mu)^T g_c + D$, where g_c is the gradient of the compliance regressor evaluated in μ and D is a constant.

This gives:

$$\log(p_\theta(x_t | x_{t+1}, v, f, l) e^{-c_\phi(x_t, v, f, l, bc)}) \approx -\frac{1}{2}(x_t - \mu)^T \Sigma^{-1}(x_t - \mu) - (x_t - \mu)^T g_c + C + D. \quad (11)$$

Hence:

$$\log(p_\theta(x_t | x_{t+1}, v, f, l) e^{-c_\phi(x_t, v, f, l, bc)}) \approx -\frac{1}{2}(x_t - \mu + \Sigma g_c)^T \Sigma^{-1}(x_t - \mu + \Sigma g_c) + \frac{1}{2} g_c^T \Sigma g_c + C + D. \quad (12)$$

The last three terms of Eq. 12 are all constant and are encapsulated in the normalizing constant Z from Eq. 8. Therefore, we have shown that $p_{\theta, \phi}(x_t | x_{t+1}, v, f, l, bc)$ can be approximated by a Gaussian with a mean shifted by $-\Sigma g_c$.

4 Empirical Evaluation

We created three datasets to train the proposed models, which are also made public to provide a standard benchmark for future research in this area.

4.1 Dataset

Diffusion model dataset The main dataset used to train, validate and test TopoDiff consists of 33000 64x64 2D images corresponding to optimal topologies for diverse input conditions. Every data sample contains six channels:

1. The first channel is the black and white image representing the optimal topology;
2. The second channel is uniform and includes the prescribed volume fraction;
3. The third channel is the von Mises stress of the full domain under the given load constraints and boundary conditions, defined as $\sigma_{vm} = \sqrt{\sigma_{11}^2 - \sigma_{11}\sigma_{22} + \sigma_{22}^2 + 3\sigma_{12}^2}$;
4. The fourth channel is the strain energy density of the full domain under the given load constraints and boundary conditions, defined as $W = \frac{1}{2}(\sigma_{11}\epsilon_{11} + \sigma_{22}\epsilon_{22} + 2\sigma_{12}\epsilon_{12})$;
5. The fifth channel represents the load constraints in the x-direction. Every node is given the value of the force applied in the x-direction on this load (0 if no force is applied on the load);
6. The sixth channel similarly represents the load constraints in the y-direction;

where $(\sigma_{11}, \sigma_{22}, \sigma_{12})$ and $(\epsilon_{11}, \epsilon_{22}, \epsilon_{12})$ are respectively the components of the stress and strain fields.

To generate every structure, we randomly selected a combination of conditions (volume fraction, boundary conditions, loads) and then computed the optimal topology using the SIMP-based TO library ToPy (Hunter et al. 2017). We defined the possible conditions in a similar way to what was done in previous works, namely: 1. The volume fraction is chosen in the interval $[0.3, 0.5]$, with a step of 0.02; 2. The displacement boundary conditions are chosen among 42 scenarios for training and 5 additional scenarios only used for testing; 3. The loads are applied on unconstrained nodes randomly selected on the boundary of the domain. The direction is selected in the interval $[0, \pi]$, with a step of $\frac{\pi}{6}$.

The main dataset is divided into training, validation, and testing as follows:

1. The **training data** consist of 30000 combinations of constraints containing 42 of the 47 boundary conditions;
2. The **validation data** consist of 200 new combinations of constraints containing the same 42 boundary conditions;
3. The **level 1 test data** consist of 1800 new combinations of constraints containing the same 42 boundary conditions;
4. The **level 2 test data** consist of 1000 new combinations of constraints containing five out-of-distribution boundary conditions.

In all test data, the combination of constraints is unseen. While *level 1* dataset contains boundary conditions that are also in the training data, we introduce more difficult conditions in *level 2* to rigorously compare TopoDiff model’s generalization ability with existing methods on a multi-level dataset.

Regressor and classifier datasets In addition to the main dataset, two other datasets are used to train the regressor and classifier needed to perform *regressor* and *classifier guidance*. A detailed description of these additional datasets is provided in the Appendix (Sec. A1).

4.2 Evaluation Metrics

Using relevant evaluation metrics is vital for every machine learning problem. It is particularly critical for mechanical design generation because most metrics used in DGMs do not correspond to the physical objective that one wants a design to achieve. In this work, contrary to most TO generative models previous works, we do not use pixel-wise error as a final evaluation metric because it does not guarantee low compliance, which is the objective we are trying to achieve.

Hence, we define and use four evaluation metrics that reflect the compliance minimization objective, as well as the constraints that the generated topologies have to respect:

1. Compliance error (CE) relative to the ground truth, defined as: $CE = (C(\hat{y}) - C(y))/C(y)$ where $C(y)$ and $C(\hat{y})$ are respectively the compliance of the ToPy-generated topology and of the topology generated by our diffusion model. It should be noted that a negative compliance error means that our model returns a topology with lower compliance than the ground truth;
2. Volume fraction error (VFE) relative to the input volume fraction, defined as: $VFE = |VF(\hat{y}) - VF(y)|/VF(y)$ where $VF(y)$ and $VF(\hat{y})$ are respectively the prescribed volume fraction and the volume fraction of the topology generated by our diffusion model;
3. Load disrespect (LD), defined as a boolean that is 1 if there is no material at a place where a load is applied and 0 if there is always material where loads are applied;
4. Presence of floating material (FM), defined as a boolean that is 1 if the topology contains floating material and 0 otherwise.

A model which generates samples with high scores on these metrics is expected to yield high-performance manufacturable designs.

4.3 Choice of hyperparameters

One of the most crucial hyperparameters is the gradient scales in our guidance strategies. These parameters quantify the relative importance of compliance minimization and floating material avoidance. As explained in Sec. 4.1, a validation dataset of 200 topologies was used to perform hyperparameter tuning. We used a grid search method to decide the hyperparameters by using compliance error and floating material presence as evaluation metrics. Topology generation and FEA were used to evaluate the results.

5 Results and Discussions

5.1 Evaluation of the full diffusion model

To evaluate the performance of TopoDiff, we use the two test sets that have been described in Sec. 4.1, corresponding to two levels of difficulty. We run every test nine times and then compute the average of the results obtained. We compare the

Test dataset	Level 1 test data			Level 2 test data		
	Model	cGAN	Unguid. TopoDiff	Guid. TopoDiff	cGAN	Unguid. TopoDiff
Average CE (%)	48.51 ± 16.38	4.10 ± 0.88	4.39 ± 0.94	143.08 ± 38.50	22.13 ± 8.52	18.40 ± 5.88
Median CE (%)	2.06	0.80	0.83	6.82	1.88	1.82
Prop. of CE >30% (%)	10.11	2.33	2.56	24.10	8.20	8.10
Average VFE (%)	11.87 ± 0.52	1.86 ± 0.03	1.85 ± 0.03	14.31 ± 0.75	1.81 ± 0.04	1.80 ± 0.04
Prop. of LD (%)	0.00	0.00	0.00	0.00	0.00	0.00
Prop. of FM (%)	46.78	6.64	5.54	67.90	7.53	6.21

Table 1: Comparison of performance between a cGAN and TopoDiff (guided and not guided) on the two level test sets. Values after \pm indicate the 95 % confidence interval around averages. The values in bold are the best ones in every row for both levels.

performance of our model on all evaluation metrics (Sec. 4.2) with a state-of-art cGAN model, TopologyGAN (Nie et al. 2021), which performs the same task as our model.

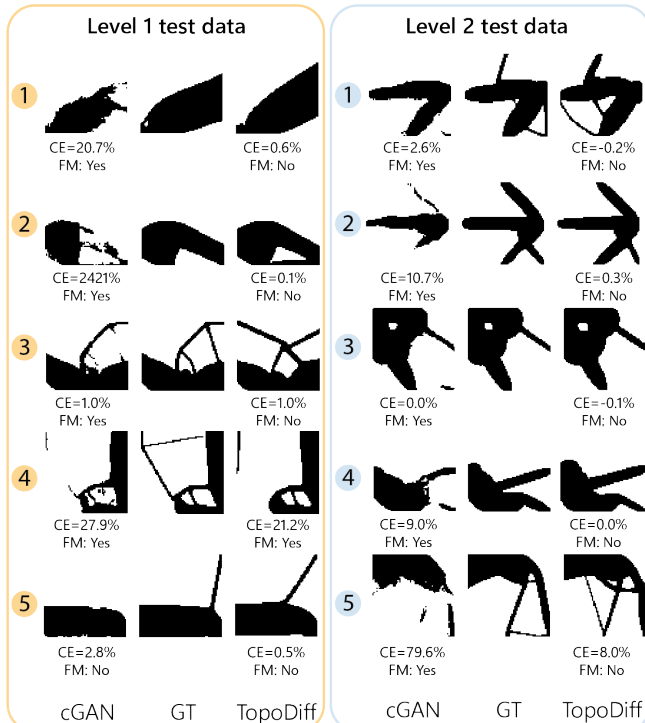


Figure 3: Comparison of generated topologies on randomly selected samples from both test datasets. GT stands for ground truth, CE is the compliance error relative to the GT, and FM indicates the presence or not of floating material.

Fig. 3 shows examples of a few topologies obtained with the SIMP method (ground truth), with the cGAN, and with TopoDiff for randomly selected constraints from *level 1* and *level 2* test sets. Qualitatively, we notice that the cGAN tries to mimic pixel-wise the topology obtained from SIMP but neglects both the compliance and the manufacturability of the generated structures, which almost all have some floating material. The topologies generated by TopoDiff, on the other hand, may visually differ more from the SIMP results but have better physical properties than cGAN. All but one of the ten TopoDiff-generated topologies have no floating material, and all ten outperform the cGAN topologies in terms

of compliance error.

To confirm these qualitative observations, Table 1 summarizes the performance of the topologies obtained with all test sets. TopoDiff outperforms cGAN on all the metrics of interest.

On the *level 1* test set, TopoDiff notably performs a reduction of the average CE by a factor of eleven and of the proportion of unmanufacturable designs thus drops from 46.8% with cGAN to 5.5% with TopoDiff. It also significantly reduces the average VFE from 11.9% to 1.9%.

On the *level 2* test set, TopoDiff achieves similar results. It performs an eight-times reduction in the average CE, from 143.1% to 18.4% and a four-times reduction in the median CE. Unmanufacturability drops from 67.9% to 6.2%, while the VFE is reduced by a factor of eight, from 14% to less than 2%. A paired one-tailed t-test confirms a reduction of the average CE and of the average VFE with a p-value of $9 \cdot 10^{-12}$ and $5 \cdot 10^{-160}$ respectively.

These results show the efficacy of diffusion models in learning to generate high-performing and manufacturable topologies for a wide set of testing conditions.

5.2 Efficiency of guidance

Surrogate models Guidance can only work if the regressors and classifiers are able to perform well, including on noisy images. Table 2 shows the performance of the compliance regressor and floating material classifier according to the level of noise. These results show that both surrogate models are very reliable on low noise topologies.

	0-25% noise	25-75% noise	75-100% noise	Global
Regressor R2 (%)	82.4	82.4	61.8	77.3
Classifier acc. (%)	98.8	76.8	54.6	76.8

Table 2: Performance (R2-score and accuracy) of both surrogate models on validation data with respect to noise level.

Ablation study To evaluate the impact of our guidance strategy on the performance of TopoDiff, we also tested it *without* guidance on the two test sets, as shown in Table 1.

With *in-distribution* boundary conditions (*level 1*), our guidance strategy has no significant impact on compliance error (both on average and median). A two-tailed paired t-test does not reject the null hypothesis ($p = 0.1$). We hypothesize that this happens because the diffusion model has

learned to perform well with these boundary conditions and does not need additional compliance guidance. In contrast, our guidance strategy significantly impacts the proportion of floating material, with decreases from 6.6% to 5.5%.

With *out-of-distribution* boundary conditions (*level 2*), the positive impact of our guidance strategy is evident both on the average compliance error and on the proportion of floating material. A paired one-tailed t-test confirms a reduction of the average CE with a p-value of 0.05. The average compliance error is reduced by 17% and the average proportion of floating material by 18%. As expected, guidance seems to have no effect on load respect and on volume fraction error. More interestingly, guidance seems to have no significant effect on the median of the compliance error, which suggests that compliance *regressor guidance* primarily reduces the number of topologies with very high compliance errors.

5.3 Limitations and future work

TopoDiff shows good performance and good generalization to out-of-distribution boundary conditions. The guidance strategy introduced is beneficial to minimizing compliance and ensuring manufacturability. However, several challenges still need to be addressed. The most significant limitation is the computation time, diffusion models being slower than GANs. It takes 0.06 seconds for TopologyGAN to generate one topology, while TopoDiff needs 21.59 seconds. It should be noted, however, that if we include the time needed to compute the physical fields that both models use as input, the relative gap is reduced: 3.37 seconds for TopologyGAN and 24.90 seconds for TopoDiff. Reducing the computation time of diffusion models has been an objective for many recent works (Ma et al. 2022a; Franzese et al. 2022; Ma et al. 2022b; Giannone, Nielsen, and Winther 2022; Lyu et al. 2022). Future works may focus on applying these methods to TO-based diffusion models. TopoDiff also shares another limitation of other deep generative models for TO, which is that it would need to be retrained if a problem with a different resolution or 3D TO problem were needed to be solved.

6 Conclusion

This work is the first attempt to use diffusion models for structural topology optimization and, more generally, to solve any physical optimization problem.

We introduced TopoDiff, a conditional diffusion model to perform topology optimization, augmented with a guidance strategy to ensure the maximization of performance and avoid unmanufacturable designs. TopoDiff achieves an eight-times reduction in the average physical compliance error and produces 11-times fewer unmanufacturable designs, compared with a state-of-art GAN. TopoDiff also achieves an eight-times reduction in volume fraction error.

Conditioning a diffusion model with constraints, training it on optimal data, and guiding it with a regressor predicting physical performance and some classifiers predicting the respect of constraints, is a general method that should allow solving similar design generation problem involving performance objectives and constraints.

Acknowledgments

The authors gratefully acknowledge the funding received from Mines Paris Foundation. They would also like to thank MISTI France for supporting this research.

References

- Amir, O.; and Sigmund, O. 2011. On reducing computational effort in topology optimization: how far can we go? *Structural and Multidisciplinary Optimization*, 44(1): 25–29.
- Amit, T.; Nachmani, E.; Shaharabany, T.; and Wolf, L. 2021. SegDiff: Image Segmentation with Diffusion Probabilistic Models. *CoRR*, abs/2112.00390.
- Behzadi, M. M.; and Ilieş, H. T. 2021. GANTL: Toward Practical and Real-Time Topology Optimization With Conditional Generative Adversarial Networks and Transfer Learning. *Journal of Mechanical Design*, 144(2). 021711.
- Bendsøe, M. P.; and Kikuchi, N. 1988. Generating optimal topologies in structural design using a homogenization method. *Computer Methods in Applied Mechanics and Engineering*, 71(2): 197–224.
- Dhariwal, P.; and Nichol, A. Q. 2021. Diffusion Models Beat GANs on Image Synthesis. In Beygelzimer, A.; Dauphin, Y.; Liang, P.; and Vaughan, J. W., eds., *Advances in Neural Information Processing Systems*.
- Franzese, G.; Rossi, S.; Yang, L.; Finamore, A.; Rossi, D.; Filippone, M.; and Michiardi, P. 2022. How Much is Enough? A Study on Diffusion Times in Score-based Generative Models.
- Giannone, G.; Nielsen, D.; and Winther, O. 2022. Few-Shot Diffusion Models.
- Guarín-Zapata, N.; and Gómez, J. 2020. SolidsPy: 2D-Finite Element Analysis with Python.
- Guo, T.; Lohan, D. J.; Cang, R.; Ren, M. Y.; and Allison, J. T. 2018. An Indirect Design Representation for Topology Optimization Using Variational Autoencoder and Style Transfer. In *2018 AIAA/ASCE/AHS/ASC Structures, Structural Dynamics, and Materials Conference, AIAA SciTech Forum*, AIAA 2018-0804.
- Ho, J.; Jain, A.; and Abbeel, P. 2020. Denoising Diffusion Probabilistic Models. *arXiv preprint arxiv:2006.11239*.
- Ho, J.; and Salimans, T. 2021. Classifier-Free Diffusion Guidance. In *NeurIPS 2021 Workshop on Deep Generative Models and Downstream Applications*.
- Hunter, W.; et al. 2017. ToPy - Topology optimization with Python. <https://github.com/williamhunter/topy>.
- Kim, G.; and Ye, J. C. 2021. DiffusionCLIP: Text-guided Image Manipulation Using Diffusion Models. *CoRR*, abs/2110.02711.
- Li, B.; Huang, C.; Li, X.; Zheng, S.; and Hong, J. 2019. Non-iterative structural topology optimization using deep learning. *Computer-Aided Design*, 115: 172–180.

- Lin, Q.; Hong, J.; Liu, Z.; Li, B.; and Wang, J. 2018. Investigation into the topology optimization for conductive heat transfer based on deep learning approach. *International Communications in Heat and Mass Transfer*, 97: 103–109.
- Lyu, Z.; XU, X.; Yang, C.; Lin, D.; and Dai, B. 2022. Accelerating Diffusion Models via Early Stop of the Diffusion Process.
- Ma, H.; Zhang, L.; Zhu, X.; and Feng, J. 2022a. Accelerating Score-based Generative Models with Preconditioned Diffusion Sampling.
- Ma, H.; Zhang, L.; Zhu, X.; Zhang, J.; and Feng, J. 2022b. Accelerating Score-based Generative Models for High-Resolution Image Synthesis.
- Meng, C.; Song, Y.; Song, J.; Wu, J.; Zhu, J.; and Ermon, S. 2021. SDEdit: Image Synthesis and Editing with Stochastic Differential Equations. *CoRR*, abs/2108.01073.
- Nichol, A.; and Dhariwal, P. 2021. Improved Denoising Diffusion Probabilistic Models. *CoRR*, abs/2102.09672.
- Nichol, A.; Dhariwal, P.; Ramesh, A.; Shyam, P.; Mishkin, P.; McGrew, B.; Sutskever, I.; and Chen, M. 2021. GLIDE: Towards Photorealistic Image Generation and Editing with Text-Guided Diffusion Models. *CoRR*, abs/2112.10741.
- Nie, Z.; Lin, T.; Jiang, H.; and Kara, L. B. 2021. TopologyGAN: Topology Optimization Using Generative Adversarial Networks Based on Physical Fields Over the Initial Domain. *Journal of Mechanical Design*, 143(3).
- Rawat, S.; and Shen, M. H. 2019. A Novel Topology Optimization Approach using Conditional Deep Learning. *CoRR*, abs/1901.04859.
- Ronneberger, O.; Fischer, P.; and Brox, T. 2015. U-Net: Convolutional Networks for Biomedical Image Segmentation. *CoRR*, abs/1505.04597.
- Rozvany, G. I. N.; Zhou, M.; and Birker, T. 1992. Generalized shape optimization without homogenization. *Structural optimization*, 4: 250–252.
- Sharpe, C.; and Seepersad, C. C. 2019. Topology Design With Conditional Generative Adversarial Networks. Volume 2A: 45th Design Automation Conference.
- Sigmund, O. 2001. A 99 Line Topology Optimization Code Written in Matlab. *Struct. Multidiscip. Optim.*, 21(2): 120–127.
- Sigmund, O.; and Maute, K. 2013. Topology optimization approaches: A comparative review. *Structural and Multidisciplinary Optimization*, 48(6): 1031–1055.
- Sohl-Dickstein, J.; Weiss, E. A.; Maheswaranathan, N.; and Ganguli, S. 2015. Deep Unsupervised Learning using Nonequilibrium Thermodynamics. *CoRR*, abs/1503.03585.
- Song, Y.; Sohl-Dickstein, J.; Kingma, D. P.; Kumar, A.; Ermon, S.; and Poole, B. 2020. Score-Based Generative Modeling through Stochastic Differential Equations. *CoRR*, abs/2011.13456.
- Sosnovik, I.; and Oseledets, I. 2019. Neural networks for topology optimization. *Russian Journal of Numerical Analysis and Mathematical Modelling*, 34(4): 215–223.
- Wang, D.; Xiang, C.; Pan, Y.; Chen, A.; Zhou, X.; and Zhang, Y. 2021. A deep convolutional neural network for topology optimization with perceptible generalization ability. *Engineering Optimization*, 54(6): 973–988.
- Yu, Y.; Hur, T.; Jung, J.; and Jang, I. G. 2018. Deep learning for determining a near-optimal topological design without any iteration. *Structural and Multidisciplinary Optimization*, 59(3): 787–799.

A1 Additional datasets used for surrogate models

The main dataset used to train, validate and test the diffusion model was presented in the paper. This section provides more information about the two other datasets that were used to train and validate the two surrogate models, namely the regressor predicting compliance and the classifier predicting the presence of floating material.

For the regressor predicting compliance, we used a dataset of 72000 labeled samples, with the label indicating the compliance of the topology under the given constraints. Every sample is an image containing eight channels (black and white topology, volume fraction, von Mises stress, strain energy density, load in x-direction, load in y-direction, x-displacement boundary condition and y-displacement boundary condition). In order to give our regressor good generalization abilities, we not only used optimal topologies (generated by SIMP), but also negative samples, corresponding to non optimal topologies. This dataset includes:

- 30000 images from the diffusion model main dataset, corresponding to *optimal topologies* (25000 for training, 5000 for validation);
- 12000 images corresponding to *non-optimal topologies*, generated using the *fake-load method*, explained below (10000 for training, 2000 for validation);
- 30000 images corresponding to *non-optimal topologies*, generated by the unguided conditional diffusion model by using the same constraints as in the main dataset (25000 for training, 5000 for validation).

It should be noted that the final dataset contains less than 72000 samples because it was filtered to remove outlier structures (with compliance higher than 50 for the first 42000 and with compliance higher than 25 for the diffusion-generated structures). To generate non-optimal structures, we notably used the *fake-load method*, which consists in adding an extra load to the input constraints given to SIMP for generating the structure. SIMP thus generates a topology that is optimal for the extra-loaded constraints but not for the real ones. This method allows to generate non-optimal data while still respecting basic requirements like the presence of material where loads are applied.

For the classifier predicting the presence of floating material, we used a dataset of 70000 labeled samples (58000 for training and 12000 for validation), with the label being a boolean indicating if floating material is present on the topology or not. Every sample is an image containing only one channel: the black and white topology. This dataset includes:

- the first 15000 images from the diffusion model main dataset, on which floating material was added;
- the first 14000 images from a dataset containing topologies at diverse volume fractions, on which floating material was added;
- the first 6000 images from the non-optimal topologies dataset generated with the *fake-load method*, on which floating material was added;
- the next 15000 images from the diffusion model main dataset, on which floating material was *not* added;
- the next 14000 images from a dataset containing topologies at diverse volume fractions, on which floating material was *not* added;

- the next 6000 images from the non-optimal topologies dataset generated with the *fake-load method*, on which floating material was *not* added.

It should be noted that while some datasets were used to train several different models, we have paid careful attention to avoiding leakage of data from training datasets to validation datasets. All models were validated on data that they had not been trained on. The final TopoDiff model (diffusion model + surrogate models) was tested on data that was never used for training or validating any of its component models.